Electronic Supplementary Material (ESI) for Soft Matter.

Combined electrokinetic and shear flows control colloidal particle distribution across microchannel cross-sections

Varun Lochab[1], and Shaurya Prakash[1*]

[1]Department of Mechanical and Aerospace Engineering, The Ohio State University, Columbus, OH 43201, USA

Corresponding Author: Shaurya Prakash
Email: prakash.31@osu.edu

Supplementary Information Text

Effect of fluid viscosity. Three different flow rates, $Q \in \{3, 6, 10\}$ μL/min over range of electric field strengths $\Delta V_{12}/L \in \{0, 20, 40, 60, 80, 100\}$ V/cm were tested for each weight fraction of glycerol. The kinematic viscosity of the Newtonian water-glycerol mixture[1, 2] more than doubles from 0.9×10^{-6} $m^2 s^{-1}$ to 2.0×10^{-6} $m^2 s^{-1}$, as glycerol fraction was changed from at 0 % (w/w) at 30 % (w/w) (Figure S1) at 25° C.

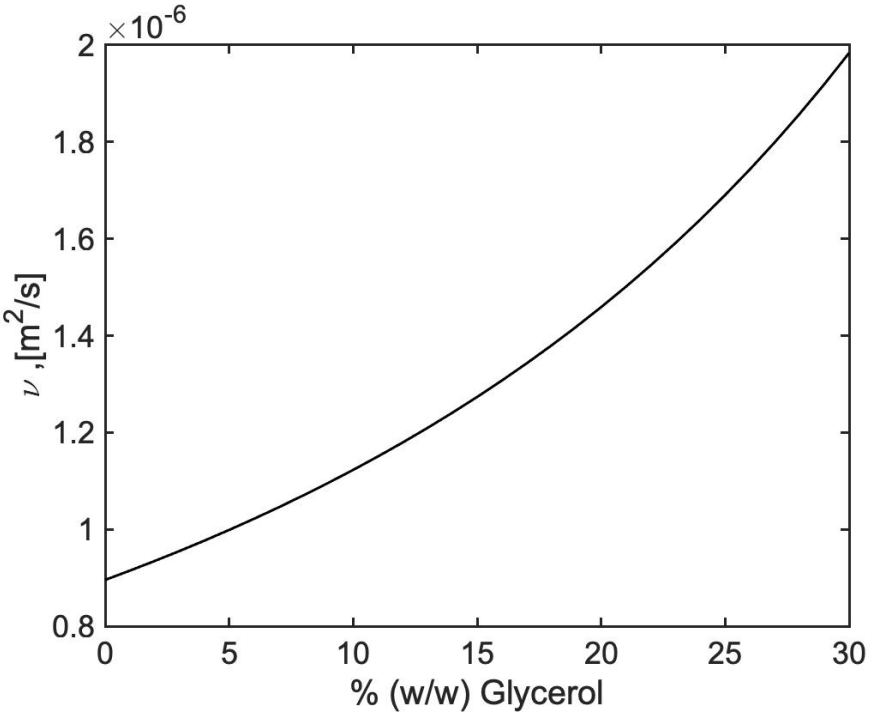

Figure S1. The fluid kinematic viscosity, υ [m^2/s] as a function of glycerol weight fraction[3] in terms of % (w/w) of water-glycerol mixtures.

Table S1. Comparison of Re_c for 0, 10, 20, 30 %(w/w) glycerol.

Flow Rate, *Q* (μL/min)	0% (w/w) Glycerol	10% (w/w) Glycerol	20% (w/w) Glycerol	30 % (w/w) Glycerol
3	0.26	0.21	0.16	0.12
6	0.53	0.42	0.32	0.24
10	0.88	0.70	0.54	0.40

The changes in electrophoretic number as a function of flow conditions are shown in Figure S2. The electrophoretic number follow the same trend as for the 0 % (w/w) glycerol; however, the magnitudes of electrophoretic number decrease as the fluid kinematic viscosity was increased. Figure S3 shows particle migration as a function of %(w/w) glycerol at 3 μL/min, 6 μL/min, and 10 μL/min.

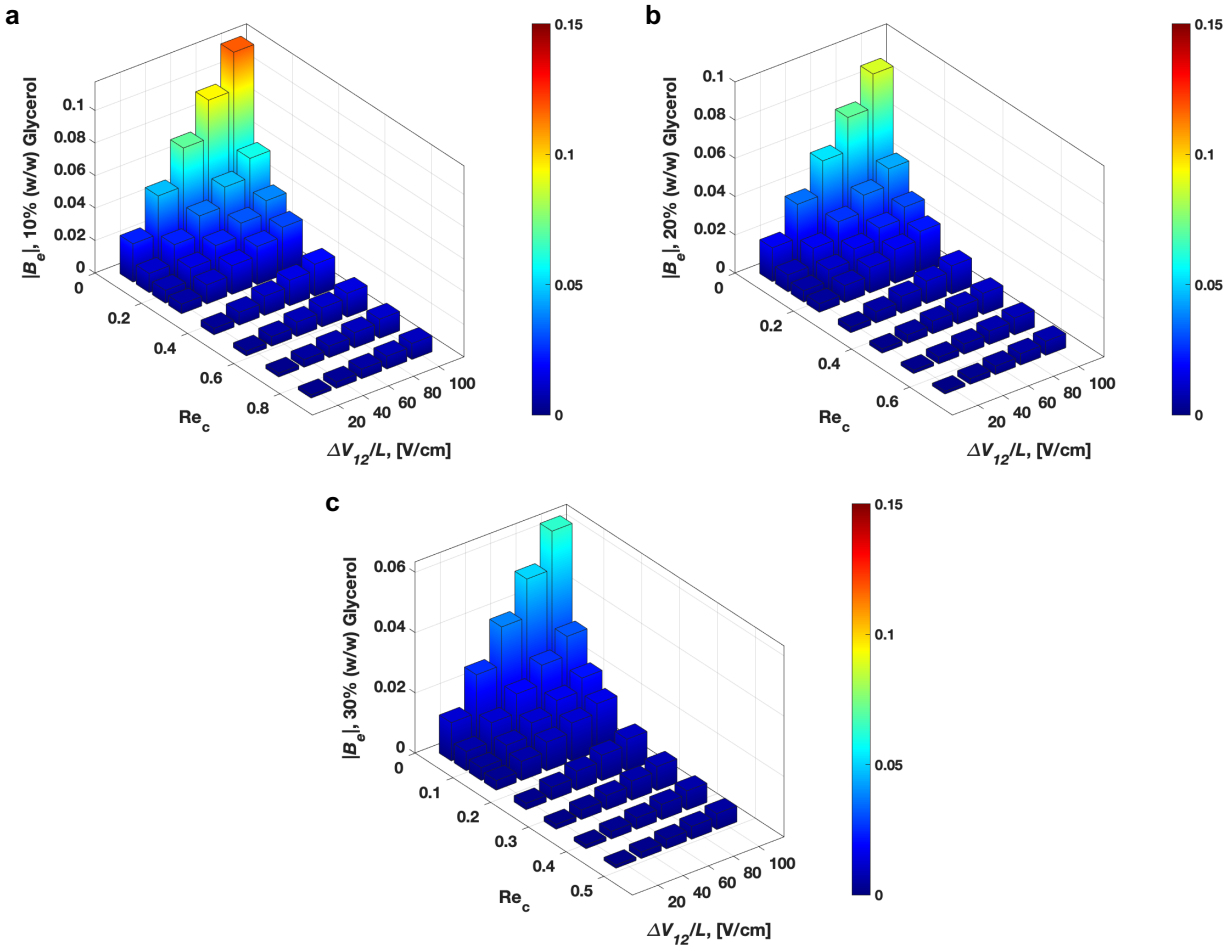

Figure S2. Electrophoretic number as a function of flow parameters. Electrophoretic number, $|B_e|$ at (a) 10% (w/w) glycerol, (b) 20% (w/w) glycerol, and (c) 30% (w/w) glycerol. The channel Reynolds numbers for the data in the plot correspond to the flow rates: 1, 2, 3, 4, 6, 8, 10, and 12 μL/min, respectively.

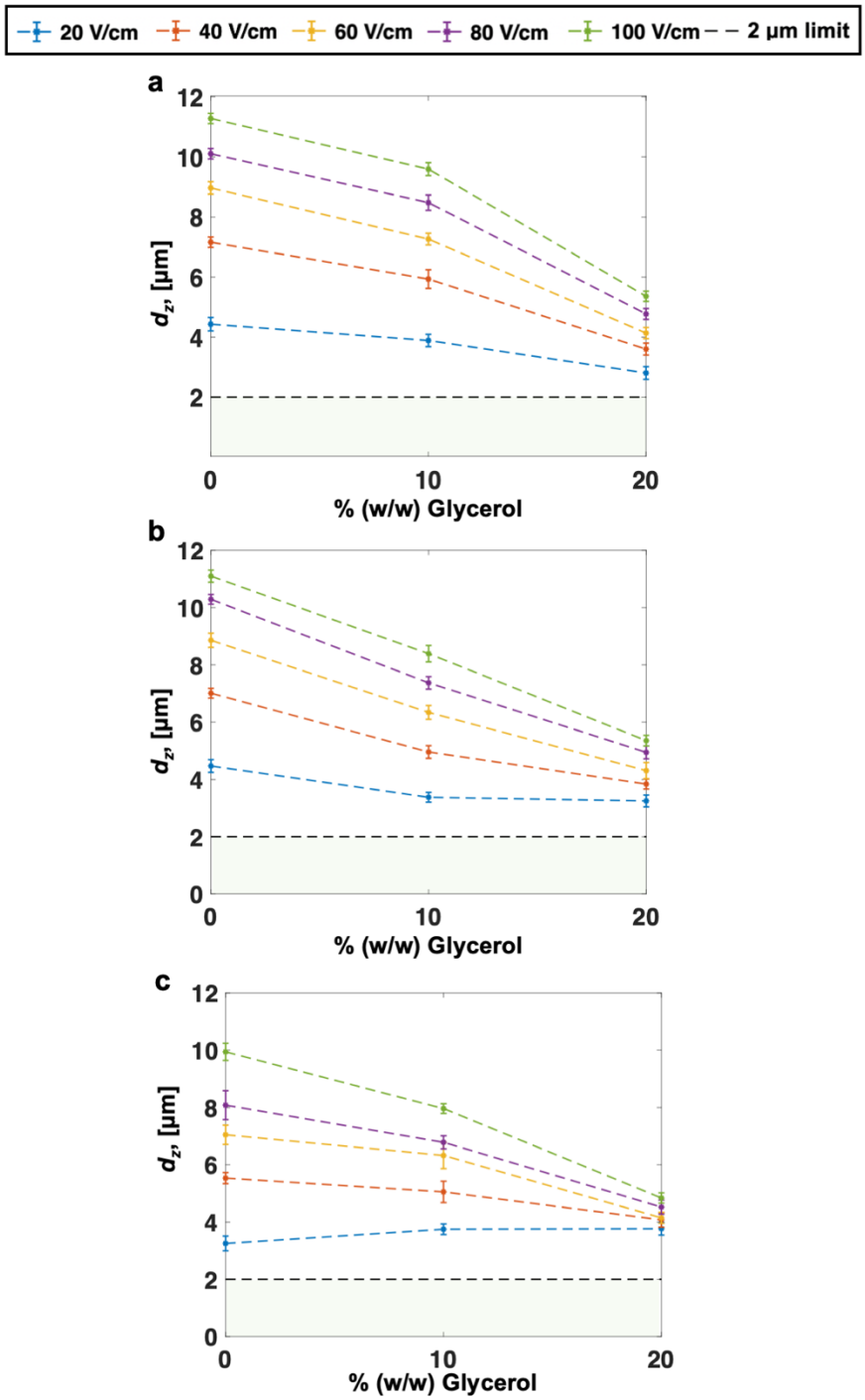

Figure S3. Effect of changing fluid viscosity at different flow rates. The width of the depletion region, d_z as a function of changing glycerol weight fraction at (a) 3 µL/min, (b) 6 µL/min, and (c) 10 µL/min show that extent of migration decreases as the kinematic viscosity is increased. Error bars represent rms variance from the mean for three measurements at each tested flow condition.

Colloidal particle migration at 0% (w/w) glycerol. The electrophoresis-induced lift forces produce a non-monotonic trend in colloidal migration, which can be seen in the confocal images presented in Figure S4, where migration was highest for the flow rate of 4 μL/min.

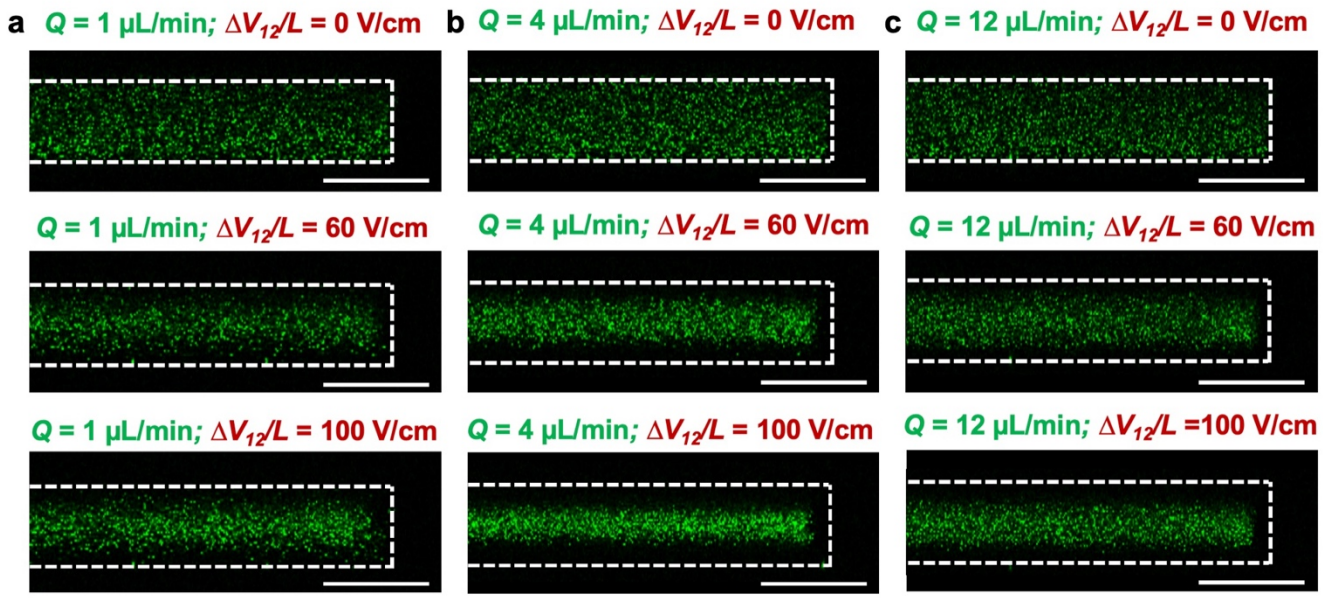

Figure S4. Confocal images showing particle migration. Cross-section views from the observation volume, where the flow direction is perpendicular to the page. A range of critical flow conditions were tested, where representative migration trends for (a) Q = 1 μL/min; (b) Q = 4 μL/min; (c) Q = 12 μL/min are shown. Note that the extent of cross-stream migration away from the top and bottom walls is on the same order of magnitude, and highest for the 4 μL/min case at both $\Delta V_{12}/L$ = 60 V/cm and $\Delta V_{12}/L$ = 100 V/cm. The scale bar is 50.00 μm.

Lift force calculation

Khair *et. al.*[4] obtained a leading order lift-force on a particle undergoing electrophoresis in inertial shear flow. The expression for this lift force was given by:

$$F_{EIL} = \frac{7\pi}{4} \frac{\varepsilon |\zeta| a^3 \rho \dot{\gamma} E_\infty}{\mu}, \tag{S1}$$

where ε = 7.08 × 10^{-10} F/m, ρ = 997 kg/m^3, and μ = 8.9 × 10^{-4} Pa•s for aqueous buffer solution. For a colloidal particle with radius, a ~ 240 nm (2.4 × 10^{-7} m), $\dot{\gamma} = 2Q/(WH^2)$, i.e. average shear (for Q = 12 μL/min, $\dot{\gamma}$ = 982 s^{-1} based on average flow velocity[4]), E_∞= 100 V/cm, the lift force ~ 10^{-17} N, or 10^{-2} fN. The calculated lift force was ~ 10^{-18} N for Q = 1 μL/min at 100 V/cm.

Estimates of migration velocities

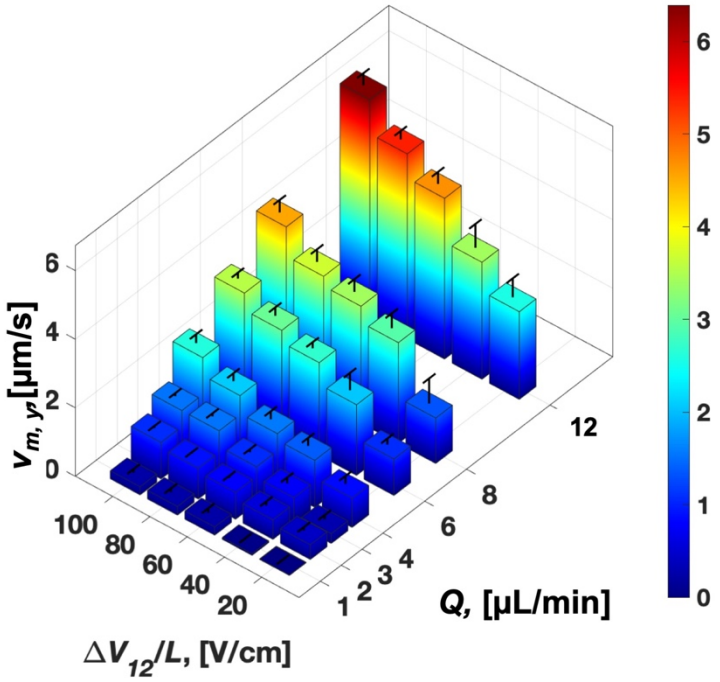

Figure S5: Estimates of migration velocity along *y* as a function of flow rate and average electric field. Error bars represent rms variance from the mean for three measurements at each tested flow condition.

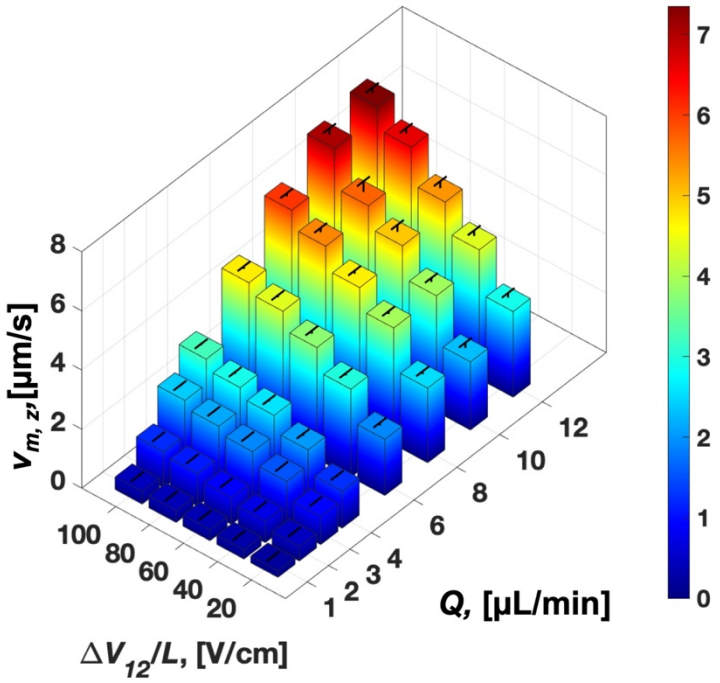

Figure S6: Estimates of migration velocity along *z* as a function of flow rate and average electric field. Error bars represent rms variance from the mean for three measurements at each tested flow condition.

Migration from side-walls. The particle migration from side-walls suggested that the lift possibly depends on local shear rate. The analytical flow profile due to background Poiseuille flow (i.e., no particles in the flow), $\bar{u}(y, z)$, is well-known[5, 6]. Figure S7a shows a contour plot for normalized (to maximum flow velocity) flow profile as a function of y/W and z/H, the magnitude of local shear rate across the channel cross-section can be defined as[6]:

$$\dot{\gamma}(y, z) = \sqrt{\left(\frac{\partial \bar{u}}{\partial y}\right)^2 + \left(\frac{\partial \bar{u}}{\partial z}\right)^2}, \tag{S2}$$

where the normalized magnitude of local shear is plotted in Figure S7b. Interestingly, if the migration magnitude in y and z (Figure 5a and 5b) i.e., d_y and d_z were normalized with channel width and height, the magnitude of normalized local shear rate was on the same order suggesting that there needs to be further evaluation of the local shear rates as described in the main manuscript.

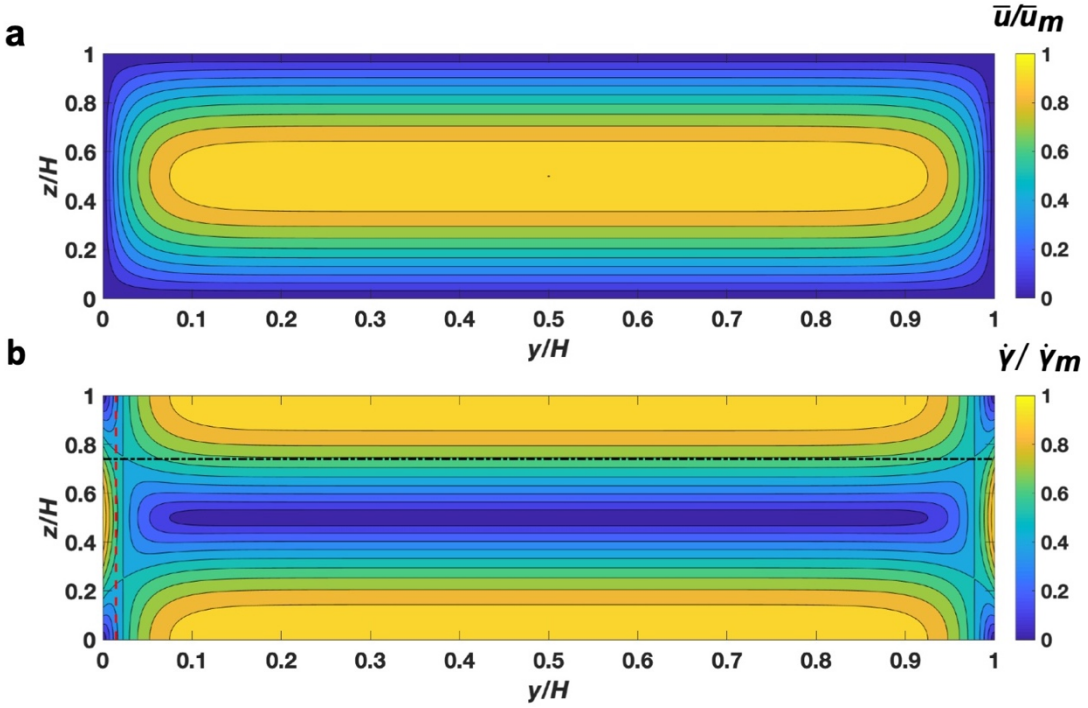

Figure S7. Flow profile and shear rate. (a) Normalized velocity profile for the background Poiseuille flow, $\bar{u}/\bar{u}_m$ for the microchannel of height, H and width, W. (b) Magnitude of normalized local shear rate, $\dot{\gamma}/\dot{\gamma}_m$, where $\dot{\gamma}_m$ is the maximum shear rate, were the same order of magnitude, i.e.,~ 0.7 times the maximum shear rate, for example, at d_y/W (red line) and d_z/H (black line) for 3 µL/min and 60 V/cm. Similar observations were seen at other flow conditions.

SI References

1. K. Mann, S. Deutsch, J. Tarbell, D. Geselowitz, G. Rosenberg and W. Pierce, *Journal of Biomechanical Engineering*, 1987, **109**, 139-147.
2. M. C. Brindise, M. M. Busse and P. P. Vlachos, *Experiments in Fluids*, 2018, **59**, 173.
3. N.-S. Cheng, *Industrial & Engineering Chemistry Research*, 2008, **47**, 3285-3288.
4. A. S. Khair and J. K. Kabarowski, *Physical Review Fluids*, 2020, **5**, 033702.
5. S. Prakash and J. Yeom, *Nanofluidics and microfluidics : Systems and applications*, Elsevier/William Andrew, Amsterdam, 2014.
6. N. Figueroa-Morales, G. Miño, A. Rivera, R. Caballero, E. Clément, E. Altshuler and A. Lindner, *Soft Matter*, 2015, **11**.